Food Analytical Methods (2022) 15:144–156
https://doi.org/10.1007/s12161-021-02095-0

Texture Profile Analysis: How Parameter Settings Affect the Instrumental Texture Characteristics of Fish Fillets Stored Under Refrigeration?

Yago Alves de Aguiar Bernardo[1,2,3,4] · Denes Kaic Alves do Rosario[2,3,5] · Maria Lúcia Guerra Monteiro[2,3,4,5] · Sérgio Borges Mano[4] · Isabella Fernandes Delgado[1] · Carlos Adam Conte-Junior[1,2,3,4,5]

Received: 13 October 2020 / Accepted: 9 July 2021 / Published online: 22 August 2021

Abstract

Texture profile analysis (TPA) is widely used to evaluate instrumental texture of fish fillets. However, different TPA setting conditions are the main limiting factor for its use as an official method of quality monitoring. Therefore, this study aimed to describe how texturometer settings affect the primary instrumental texture properties of Nile tilapia (*Oreochromis niloticus*) fillets stored at 4.0 °C for 8 days. Different settings were employed, including compression rate (CR) between 43.2 and 76.8%, holding time (HT) between 0.1 and 10 s, and test speed (TS) between 0.3 and 3.7 mm/s, applying the central composite rotatable design (CCRD). The CR affected all properties throughout storage. CR and TS similarly influenced cohesiveness and resilience, forming stability zones at CR values above 67% and TS values below 2 mm/s. HT changed springiness linearly, quadratically and by interactions, and the stability was achieved at HT values below 5 s. These findings suggest that in the range of 60–75% (CR), 2–5 s (HT), and 0.5–2.0 mm/s (TS), it is possible to obtain more representative results for the instrumental texture properties.

Keywords Central composite rotatable design · Response surface methodology · TPA · Instrumental texture parameters · Mechanical properties · Storage

Introduction

Texture is one of the main parameters for physical evaluation of fish quality for producers and consumers (Singh and Benjakul 2018). Elegant studies have been published evaluating how the fish texture changes through the degradation process (Monteiro et al. 2019; Rodrigues et al. 2017), and the most recent articles employed the instrumental texture or texture profile analysis (TPA) as an assessment method (Jiang et al. 2018; Li et al. 2018; Sun et al. 2018; Roco et al. 2018; Wu et al. 2018; Pavón et al. 2018; Sreelakshmi et al. 2019; Cropotova et al. 2019; Monteiro et al. 2019; Harimana et al. 2019; Wang et al. 2019; Tang et al. 2019; Bruni et al. 2020; Boughattas et al. 2020). TPA is applied to mimic what occurs inside the mouth, allowing to obtain a force–time curve through two sample compression cycles, meaningful to identify some texture properties of food (Nishinari et al. 2019). The idea of performing "two bites" through two successive compression cycles obtained with a cylindrical probe was firstly described by Bourne (1968) in one of the pioneering studies in the area. However, the two compression cycles were the only setting that has remained constant since the first methodologies were described (Nishinari et al.

✉ Carlos Adam Conte-Junior
conte@iq.ufrj.br

1 Graduate Program in Sanitary Surveillance (PPGVS), National Institute of Health Quality Control (INCQS), Oswaldo Cruz Foundation (FIOCRUZ), Rio de Janeiro, RJ 21040-900, Brazil

2 Center for Food Analysis (NAL), Technological Development Support Laboratory (LADETEC), Federal University of Rio de Janeiro (UFRJ), Cidade Universitária, Rio de Janeiro, RJ, Brazil

3 Laboratory of Advanced Analysis in Biochemistry and Molecular Biology (LAABBM), Department of Biochemistry, Federal University of Rio de Janeiro (UFRJ), Cidade Universitária, Rio de Janeiro, RJ 21941-909, Brazil

4 Graduate Program in Veterinary Hygiene (PPGHV), Faculty of Veterinary Medicine, Fluminense Federal University (UFF), Vital Brazil Filho, Niterói, RJ 24230-340, Brazil

5 Graduate Program in Food Science (PPGCAL), Institute of Chemistry (IQ), Federal University of Rio de Janeiro (UFRJ), Cidade Universitária, Rio de Janeiro, RJ 21941-909, Brazil

2019). Moreover, although the most recent studies standardize mechanical issues such as sample geometry and dimensions, they present a wide range of variations, including the compression rate (CR) (25–80%), the interval between cycles or holding time (HT) (1–60 s), and the test speed (TS) (0.2–10 mm/s) (Table 1). An example of the lack of standardization of the methodology can be observed when comparing the results obtained for hardness of tilapia fillets (*Oreochromis niloticus*) in Monteiro et al.'s (2019) and Wu et al.'s (2018) work. The authors evaluated the effects of UV-C radiation and high hydrostatic pressure (HHP), and stocking density on the texture of the fillets, respectively. However, Monteiro et al. (2019) applied 50% of CR, while Wu et al. (2018) applied 70% of CR. Thus, when comparing the results achieved by these authors (42.59 N and 14.37 N, respectively), it becomes difficult to conclude whether the different responses are related to the treatments performed in the studies (UV-C and HHP use, or stocking density) or the non-standardized conditions for instrumental texture evaluation. Therefore, different setting conditions could be supposedly responsible for different texture results for the same sample (Peleg 2019), representing the main limitation for the use of TPA as an assessment method of fish quality.

Table 1 Recent texture profile analysis protocols used for fish texture evaluation

Fish species	Compression rate (%)	Holding time (s)	Test speed (mm/s)	References
Sturgeon (*Acipenser gueldenstaedtii*)	40	5	Pre-test:1 Test: 1 Post-test: 10	Boughattas et al. 2020
Salmon (*Salmo salar*)	50	ND	Both: 0.5	Bruni et al. 2020
Grass carp (*Ctenopharyngodon idella*)	60	5	Both: 2	Cheng et al. 2017
Mackerel (*Scomber scombrus*)	40	5	Both: 1	Cropotova et al. 2019
Carpa (*Cyprinus carpio*)	50	5	Both: 2	Durmuş et al. 2017
Bass (*Micropterus salmoides*)	25	ND	Both: 1	Harimana et al. 2019
Sea bream (*Pagellus bogaraveo*)	50	ND	Both: 0.5	Iaconisi et al. 2017
Bighead carp (*Aristichthys nobilis*)	70	5	Pre-test: 1 Test: 3 Post-test: 5	Jiang et al. 2018
Five emerging fish species*	75	ND	Both: 1	Lazo et al. 2017
Turbot (*Scophthalmus maximus*)	60	5	Pre-test: 2 Test: 1 Post-test: 1	Li et al. 2018
Seabass (*Lateolabrax japonicus*)	60	30	Both: 0.8	Liang et al. 2017
Grass carp (*Ctenopharyngodon idella*)	30	5	Pre-test: 1 Test: 1 Post-test: 5	Lin et al. 2012
Tilapia (*Oreochromis niloticus*)	50	5	Both: 1	Monteiro et al., 2019
Pacu (*Piaractus mesopotamicus*)	50	5	Both: 2	Pavón et al. 2018
Ruff (*Seriolella violacea*)	50	10	Both: 2	Roco et al. 2018
Five Brazilian fish species**	60	15	Pre-test: 1 Test: 1 Post-test: 5	Rodrigues et al. 2017
Puffer fish (*Lagocephalus guentheri)*	40	ND	Both: 0.2	Sreelakshmi et al. 2019
Mandarin fish (*Siniperca chuatsi*)	30	ND	Both: 1	Sun et al. 2018
Mandarin fish (*Siniperca chuatsi*)	80	60	Both: 1	Tang et al. 2019
Fresh crucian carp	70	ND	Both: 1	Wang et al. 2019
Tilapia (*Oreochromis niloticus*)	70	ND	Both: 1	Wu et al. 2018
Turbot (*Psetta maxima*)	50	ND	Both: 1	Xu et al. 2016
Grass carp (*Ctenopharyngodon idella*)	ND	ND	Both: 0.5	Yang et al. 2015

ND Not described

*Meagre (*Argyrosomus regius*), greater amberjack (*Seriola dumerili*), pikeperch (*Sanders lucioperca*), wreckfish (*Polyprion americanus*), and grey mullet (*Mugil cephalus*)

**Pintado (*Pseudoplatystoma corruscans*), piau (*Leporinus freiderici*), tucunaré (*Cichla ocellaris*), curimbatá (*Prochilodus lineatus*), and matrinxã (*Brycon cephalus*)

As described by Rosenthal (2010), a texture analyzer is able to measure fish instrumental texture primary properties (e.g., hardness and cohesiveness). However, recently, hardness, springiness, cohesiveness, resilience, and chewiness are the most commonly accepted and studied properties for fish texture evaluation (Iaconisi et al. 2017; Rodrigues et al. 2017; Sun et al. 2018; Cropotova et al. 2019; Monteiro et al. 2019; Wang et al. 2019; Tang et al. 2019; Bonfim et al. 2020). Hardness was originally defined as the force required to obtain a given deformation (Nishinari and Fang 2018), which in practice corresponds to the peak force achieved by the first uniaxial compression cycle ("first bite") (Fig. 1). In this way, the application of different CRs is suspect in resulting in different hardness values for similar samples (Peleg 2019). Therefore, the same problem seems to affect the results of resilience and cohesiveness, or "structural recoverability" (Nishinari and Fang 2018), since they correspond to the ratio of upstroke area to downstroke area of the first cycle and to the ratio of the areas under the "two bites" peaks, respectively. Moreover, these two primary properties are both affected by the TS (Rosenthal 2010), as this must mimic the speed of human chewing (Nishinari et al. 2019). Also, springiness appears to be affected by the holding time since this is a ratio between the time to start the second compression and the time to reach the second peak (Sun et al. 2018). Finally, chewiness is a secondary instrumental property, resulting from the product of hardness, cohesiveness, and springiness (Sun et al. 2018), and defined as the energy required to masticate a solid food product to a state ready for swallowing (Nishinari and Fang 2018). In this way, the influences exerted by the texturometer parameters have an indirect effect on this property, making it essential to assess the responses of the primary properties, which seem to be directly affected by the variations in the texture profile analysis settings.

Instrumental texture properties are known as a potential quality index for fish species; however, the lack of analytical standardization toward parameter settings, including the understanding of their interactions (dependency relationship), leads to findings highly variable in the literature, representing a gap for application of this methodology as an instrumental method for assessing the quality of fish. It is remarkable that there are no studies in the scientific literature that investigate significant ranges of TPA configuration parameters in fish and their consequences in the data. Therefore, the aim of this study was to evaluate the effects of the compression rate, holding time, and test speed on the primary instrumental texture properties (hardness, springiness, cohesiveness, and resilience) of Nile tilapia (*Oreochromis niloticus*) fillets, the third most farmed fish species worldwide (FAO 2020). For this purpose, the design of experiments (DoE) approach was employed to obtain a mathematical model that describes the effects (linear, quadratic, and interactions) of these three factors in achieving the TPA.

Material and Methods

Experimental Design

A central composite rotatable design (CCRD) experiment was used in a 2^3 experiment (Table 2). CCRD was initially developed by Box and Wilson (1951), and according to Aslan (2008) it provides as much data as a complete factorial design but requires less analysis. The number of treatments necessary to compose a CCRD is defined by using Eq. (1). Therefore, this study was composed of eight factorial points and six axial points, and five replicates in the central point were used to evaluate the experimental error and the lack-of-fit of the model. A total of 19 treatments (Table 2) were performed in random order to assess the effects of compression rate (CR), holding time (HT), and test speed (TS) in the texture profile analysis (TPA) of Nile tilapia fillets. The central (0) and intermediate (− 1 and + 1) levels were determined according to the most common values found in the literature (Table 1). The *Statistica* 10© software was used for the complete statistical analysis by using the "experimental design (DOE)" function, "central composite, non-factorial,

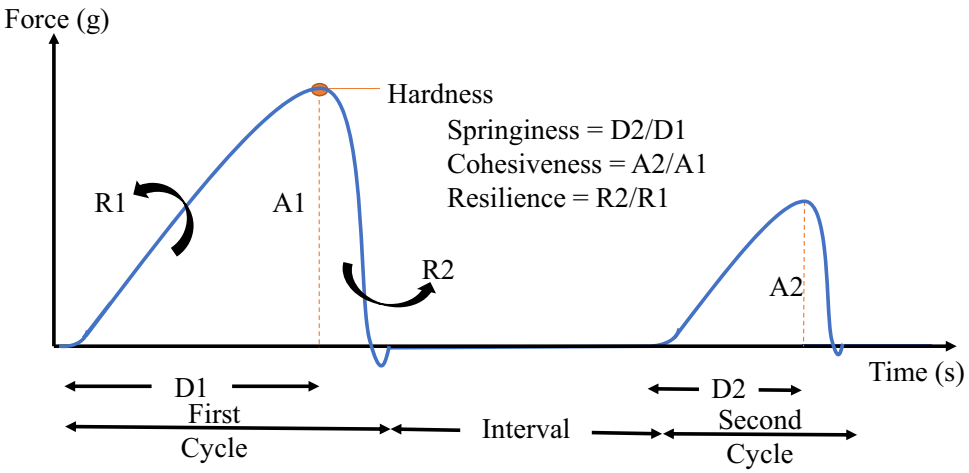

Fig. 1 Typical instrumental TPA force–time deformation curve with slight modifications. A1, area under the curve for the first compression. A2, area under the curve for the second compression. D1, time or distance between the start of the first cycle and the first peak force. D2, force or distance between the start of the second cycle and the second peak force. R1, area under the curve for the first compression downstroke. R2, area under the curve for the first compression upstroke

Table 2 Texture profile analysis treatments and factors (independent variables) and levels coded and not coded, according to central composite rotatable design

Treatments	CR (%)	HT (s)	TS (mm/s)
1	50 [−1]	2 [−1]	1 [−1]
2	50 [−1]	2 [−1]	3 [+1]
3	50 [−1]	8 [+1]	1 [−1]
4	50 [−1]	8 [+1]	3 [+1]
5	70 [+1]	2 [−1]	1 [−1]
6	70 [+1]	2 [−1]	3 [+1]
7	70 [+1]	8 [+1]	1 [−1]
8	70 [+1]	8 [+1]	3 [+1]
9	43.2 [−1.68]	5 [0]	2 [0]
10	76.8 [+1.68]	5 [0]	2 [0]
11	60 [0]	0.1 [−1.68]	2 [0]
12	60 [0]	10 [+1.68]	2 [0]
13	60 [0]	5 [0]	0.3 [−1.68]
14	60 [0]	5 [0]	3.7 [+1.68]
15	60 [0]	5 [0]	2 [0]
16	60 [0]	5 [0]	2 [0]
17	60 [0]	5 [0]	2 [0]
18	60 [0]	5 [0]	2 [0]
19	60 [0]	5 [0]	2 [0]

Values in square brackets are coded variables

CR compression rate, *HT* holding time, *TS* test speed

surface designs" option, and "3/1/16" design to obtain the 19 treatments.

$$\text{CCRD treatments} = 2^k + 2k + n \quad (1)$$

wherein k is the number of factors, and n is the number of central point replicates.

Sample Preparation

A total of 114 fresh Nile tilapia (*Oreochromis niloticus*) fillets were purchased from a local fish market in Niterói, Brazil (latitude 22° 56′ 29.2″ S and longitude 43° 03′ 17.4″ W) on the slaughter day (day 0) and transported to the laboratory in ice chests at 4 °C. The tilapia fillets were weighed (211.3 ± 31.7 g), measured (18.8 ± 1.3 cm length, 10.4 ± 0.8 cm width, and 2.0 ± 0.2-cm thickness), and randomly divided into three groups (days 0, 4, and 8) of 38 fillets. The tilapia fillets were then packed in polystyrene trays covered with oxygen-permeable polyvinyl-chloride film and stored at 4.0 ± 0.1 °C.

Instrumental Texture Evaluation

Texture profile analysis (TPA) was measured using a TA.XTplus Texture Analyzer (Stable Micro System, Godalming, UK) equipped with a 5-kg load cell. The whole experiment was performed at room temperature (20 ± 2 °C), applying a cylindrical P/36R probe, strain as target mode, auto (force) as trigger type, and 5 g of trigger force. On each storage day, each treatment was applied to two fillets, and each sample was compressed on four different points, as illustrated in Fig. 2, to obtain an average value for each property. The compression rate, holding time, and test speed of the treatments are presented in Table 2.

The following are the instrumental texture properties: (i) hardness (N), peak force required to compress samples at first downstroke (Casas et al. 2006); (ii) springiness, the ratio of time or distance between the second downstroke (D2) and the first downstroke (D1); (iii) cohesiveness, or structural recoverability of the sample (Nishinari et al. 2019), measured as the ratio of the positive force during the second compression (A2) to the positive force during the first compression (A1); and (iv) resilience, the ratio of the upstroke area (R2) to the downstroke area (R1) during the first compression cycle (Iaconisi et al. 2017), where all of them were determined from the resulting force–time curve (Fig. 1). The Exponent software package, version 6.1.9.1 (Stable Micro Systems, Surrey, England), was used to calculate both characteristics.

Mathematical Modeling

Second-order polynomial equations (Eq. (2)) (Baş and Boyacı 2007) were obtained to describe the effects of the independent variables (CR, HT, and TS) on the instrumental texture properties (hardness, springiness, cohesiveness, and resilience), maintaining only the significant terms ($p < 0.05$). The graphical model representation of the obtained models was assessed by the response surface methodology (RSM). Mean square error (MSE), lack-of-fit (LOF), and the adjusted coefficient of determination (R^2_{adj}) were calculated to verify the goodness-of-fit. Shapiro–Wilk's test was used to validate the normality of the residual data.

wherein X is the variable (CR, HT, or TS), B is the regression coefficient, and ε is the experimental error.

$$\text{Instrumental texture parameter} = B_0 + \sum_{i=1}^{3} BiXi + \sum_{i=1}^{3} B_{ii}X^2 + \sum_{i=1}^{2} \sum_{j>i}^{3} B_{ij}X_iX_j + \varepsilon \quad (2)$$

Model Validation

The model validation was evaluated through the accuracy factor (A_f) and the bias factor (B_f) (Eqs. (3) and (4)), both calculated as described by Baranyi et al. (1999), where *Af* indicates the spread of data around the prediction, and *Bf* indicates the level of agreement between predicted and observed values (Rosario et al. 2019; Baranyi et al., 1999). For this purpose, eight additional experiments were performed (Table 3), in which the tested conditions (random) were not used for the construction of the models.

$$A_f = \exp\left(\sqrt{\frac{\sum_{k=1}^{m}(\mathrm{Ln}f(x^k) - \mathrm{Ln}\mu^k)^2}{m}}\right) \quad (3)$$

$$B_f = \exp\left(\frac{\sum_{k=1}^{m}(\mathrm{Ln}f(x^k) - \mathrm{Ln}\mu^k)}{m}\right) \quad (4)$$

wherein Ln $f(x)$ is the value predicted by the model, Ln μ is the observed value, and m is the number of experiments.

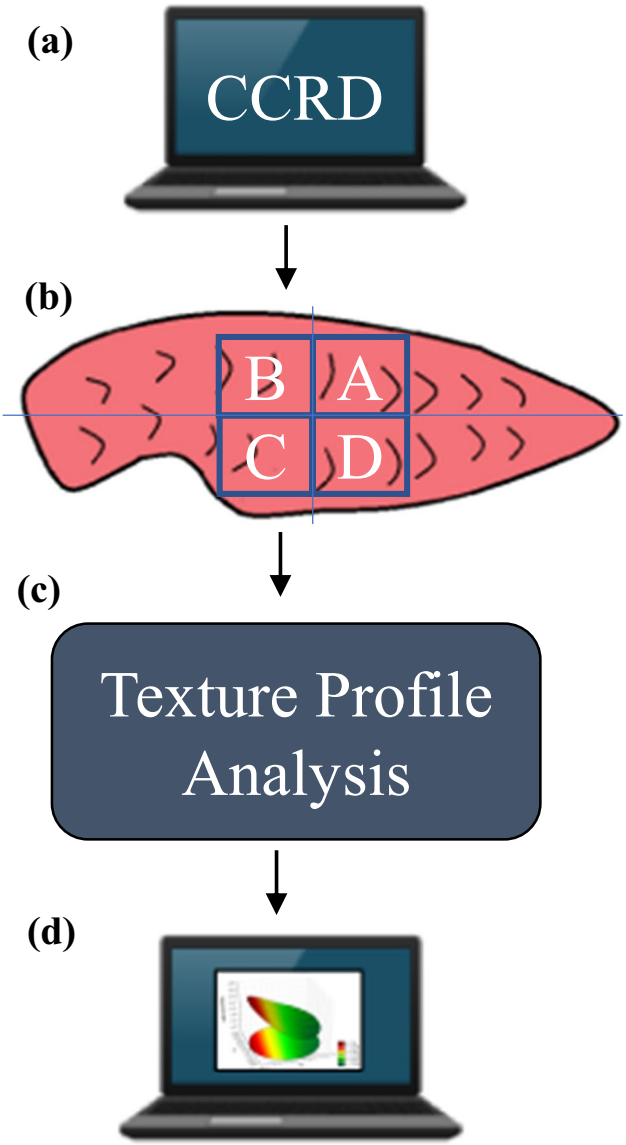

Fig. 2 Analytical flowchart. **a** Firstly, the experimental design was developed using the central composite rotatable design in a 2^3 experiment, considering the compression rate, holding time, and test speed as factors, resulting in 19 treatments for each day (0, 4, and 8). **b** The 114 Nile tilapia fillets were purchased, totaling 38 fillets for each day of analysis (two for each of the treatments). Each fillet was divided into four sites (A, B, C, and D) around the central point for the textural assessment. **c** The TPA results (hardness, springiness, cohesiveness, and resilience) for each treatment were the average value obtained by the evaluation of the four sites of two independent replicates. **d** The results obtained by each CCRD run were used to develop the response surfaces, and the mathematical models were evaluated by their performance (R^2_{adj}, MSE, and LOF values) and validated (*Af* and *Bf* factors) according to the additional random treatments

Results and Discussions

Model Performance and Mathematical Validation

The instrumental texture of Nile tilapia fillets stored at 4° C was significantly affected by all factors ($p < 0.05$), as depicted in Table 4, in which the equations for each property in the 3 days of storage are shown. Both equations were modeled by multiple regression analysis, maintaining only the significant terms ($p < 0.05$). The Shapiro–Wilk test, applied to verify the normality of the residual values (Granato et al. 2014), showed that the residues of all models were normally distributed (Table 5) ($p > 0.05$).

The performance indices used to assess the goodness-of-fit for the models are displayed in Table 5. The R^2_{adj} for every model was higher than 0.76 and less than 0.98, indicating an adequate explanation for the variability of

Table 3 Additional experiments for validation of the model for texture profile analysis using different compression rates, holding times, and test speeds

Treatments	CR (%)	HT (s)	TS (mm/s)
1	75	9	0.5
2	71	6	3.25
3	67	3	1.25
4	63	0.5	3.5
5	59	4	0.75
6	55	9.5	1.75
7	51	1	2.75
8	47	7	2.25

CR compression rate, *HT* holding time, *TS* test speed

Table 4 Polynomial models (Eqs. (5), (6), (7), (8), (9), (10), (11), (12), (13), (14), (15), and (16)) for instrumental texture properties in tilapia fillets stored at 4.0 ± 0.1 °C for 8 days

Instrumental properties	
Day 0	
Hardness (Newton)	$-72.443 + 2.995 \bullet CR$ (5)
Springiness (ratio)	$0.68 + 0.0006 \cdot CR - 0.0018 \cdot HT^2 + 0.0304 \cdot TS + 0.000238 \cdot CR \cdot HT$ (6)
Cohesiveness (ratio)	$1.315 - 0.0272 \cdot CR + 0.000174 \cdot CR^2 + 0.01325 \cdot TS$ (7)
Resilience (ratio)	$0.84 - 0.0203 \cdot CR + 0.000134 \cdot CR^2 + 0.000078 \cdot HT^2 + 0.01027 \cdot TS$ (8)
Day 4	
Hardness (Newton)	$-13.896 + 1.205 \cdot CR + 1.887 \cdot HT + 16.545 \cdot TS - 1.39 \cdot HT \cdot TS$ (9)
Springiness (ratio)	$0.5466 + 0.004367 \cdot CR + 0.01758 \cdot TS$ (10)
Cohesiveness (ratio)	$1.0861 - 0.01997 \cdot CR + 0.000117 \cdot CR^2 + 0.014168 \cdot TS$ (11)
Resilience (ratio)	$0.65831 - 0.015 \cdot CR + 0.000093 \cdot CR^2 + 0.00902 \cdot TS$ (12)
Day 8	
Hardness (Newton)	$214.861 - 5.473 \cdot CR + 0.0478 \cdot CR^2 - 1.181 \cdot HT - 26.761 \cdot TS + 0.583 \cdot CR \cdot TS$ (13)
Springiness (ratio)	$-0.2351 + 0.0285 \cdot CR - 0.000191 \cdot CR^2 + 0.0000177 \cdot HT^2 + 0.216638 \cdot TS - 0.025335 \cdot TS^2 - 0.0000413 \cdot CR \cdot HT - 0.00165 \cdot CR \cdot TS$ (14)
Cohesiveness (ratio)	$1.20811 - 0.02342 \cdot CR + 0.0001414 \cdot CR^2 + 0.016139 \cdot TS$ (15)
Resilience (ratio)	$0.66643 - 0.015376 \cdot CR + 0.000096 \cdot CR^2 - 0.001312 \cdot HT + 0.012844 \cdot TS$ (16)

the data. The LOF was not significant for both models ($p < 0.05$), strongly suggesting a good fit, since this term is calculated using the error variance, independently of the model predictions (Smith and Rose 1995). Besides, the models presented a low MSE, which represents the variability that remains in the model, including the natural variability of the experiment and systematic errors (te Giffel and Zwietering 1999).

The accuracy factor (*Af*) and bias factor (*Bf*) were measured for each property for each day of storage through the eight additional treatments (Table 5). *Af* values ranged between 1.000 and 1.052, similar to those presented by *Bf*. This range of values of *Af* indicates that predicted and observed values are in well agreement, as closer to 1.00 (perfect fit); fewer data is disseminated around the prediction (Ross 2000; Patras et al. 2009). Also, *Bf* values between 0.9 and 1.05 could be considered good, as *Bf* indicates the degree of over or under prediction exhibited by the model, as described by Ross (2000). Therefore, considering the performance and validation, the obtained models explain the

Table 5 Distribution normality and model performance tests of texture profile analysis in tilapia fillets stored at 4.0 ± 0.1 °C for 8 days

Days	Properties	Residual distribution normality*	R^2_{adj}	LOF	MSE	*Af*	*Bf*
0	Hardness (Newton)	Normal (0.645)	0.86	0.49	92.79	1.010	1.035
	Springiness (ratio)	Normal (0.152)	0.81	0.26	< 0.001	1.003	1.021
	Cohesiveness (ratio)	Normal (0.665)	0.85	0.1	< 0.001	1.012	1.004
	Resilience (ratio)	Normal (0.9)	0.91	0.087	< 0.001	1.021	1.052
4	Hardness (Newton)	Normal (0.053)	0.87	0.165	11.7	1.000	1.009
	Springiness (ratio)	Normal (0.469)	0.77	0.53	< 0.001	1.003	1.020
	Cohesiveness (ratio)	Normal (0.219)	0.93	0.43	< 0.001	1.011	1.004
	Resilience (ratio)	Normal (0.509)	0.92	0.39	< 0.001	1.052	1.082
8	Hardness (Newton)	Normal (0.298)	0.97	0.72	8.19	1.000	1.000
	Springiness (ratio)	Normal (0.878)	0.9	0.47	< 0.001	1.003	1.016
	Cohesiveness (ratio)	Normal (0.893)	0.93	0.35	< 0.001	1.005	1.025
	Resilience (ratio)	Normal (0.961)	0.94	0.07	< 0.001	1.002	1.005

*p values obtained by the Shapiro–Wilk tests. *Af* accuracy factor, *Bf* bias factor, *LOF* lack-of-fit, *MSE* mean square error, R^2_{adj} adjusted coefficient of determination

effects of CR, HT, and TS on TPA of fish fillets with high accomplishment.

Day 0

The results obtained at this storage point are due to the first biochemical changes that occur after the death of the animal. As described by Borges et al. (2013), fish fillets at this time present good microbiological quality due to the pH around 6, which hinders the development of spoilage microorganisms. This pH is due to lactic acid production via anaerobic glycolysis due to the absence of muscle oxygen at this stage. However, adenosine triphosphate (ATP) is required to separate the actin-myosin cross-bridges during the muscular relaxation in vivo, and due to the oxygen absence, ATP levels are depleted, resulting in sarcomere shortening and subsequent rigor mortis (Moriya et al. 2019). Thus, the values of hardness and springiness are expected to be the highest and the lowest at this stage, respectively.

The linear effect of CR was significantly positive for the four primary properties of instrumental texture (Table 6) ($p < 0.05$). The hardness values were the highest in this storage period, similar to the results described by Monteiro et al. (2019) for Nile tilapia (*Oreochromis niloticus*). Moreover, hardness was significantly affected only by CR (linearly) ($p < 0.05$). Since hardness is displayed as the peak force of the first compression (Fig. 1), HT and TS were not expected to be significant factors. Springiness was the only property significantly affected by the interaction between two factors (CR and HT) and by the negative quadratic effect of HT (Table 6) ($p < 0.05$). Moreover, HT (linear) and TS (quadratic) were marginally negatively significant ($p < 0.10$). Thus, HT seems to be the most sensitive factor for determining instrumental springiness. HT values above 5 s determine quadratic reductions in the results obtained for springiness. Therefore, it is possible to state that HT values between 1 and 6 s are the most suitable for texture analysis at the beginning of storage (Table 7). Also, in the range between 1

Table 6 Effects estimates for instrumental texture in tilapia fillets stored at 4.0 ± 0.1 °C for 8 days

Day		Factor									
0		**Intercept**	**CR**	**HT**	**TS**	**CR²**	**HT²**	**TS²**	**CR·HT**	**CR·TS**	**HT·TS**
Hardness (Newton)	**EE**	107.28	59.91	NS	NS	NS	NS	NS	NS	NS	NS
	SE	2.21	5.21	-	-	-	-	-	-	-	-
Springiness (ratio)	**EE**	0.808	0.035	NS	0.06	NS	−0.046	NS	−0.029	NS	NS
	SE	0.004	0.007	-	0.007	-	0.007	-	0.009	-	-
Cohesiveness (ratio)	**EE**	0.337	–0.126	NS	0.026	0.034	NS	NS	NS	NS	NS
	SE	0.004	0.007	-	0.007	0.007	-	-	-	-	-
Resilience (ratio)	**EE**	0.122	–0.084	NS	0.02	0.028	0.012	NS	NS	NS	NS
	SE	0.002	0.003	-	0.003	0.003	0.003	-	-	-	-
4		**Intercept**	**CR**	**HT**	**TS**	**CR²**	**HT²**	**TS²**	**CR·HT**	**CR·TS**	**HT·TS**
Hardness (Newton)	**EE**	87.02	24.1	−5.36	19.18	NS	NS	NS	NS	NS	–8.34
	SE	0.78	1.85	1.85	1.85	-	-	-	-	-	2.41
Springiness (ratio)	**EE**	0.843	0.087	NS	0.035	NS	NS	NS	NS	NS	NS
	SE	0.005	0.011	-	0.011	-	-	-	-	-	-
Cohesiveness (ratio)	**EE**	0.339	–0.117	NS	0.028	0.023	NS	NS	NS	NS	NS
	SE	0.004	0.007	-	0.007	0.007	-	-	-	-	-
Resilience (ratio)	**EE**	0.107	–0.078	NS	0.018	0.018	NS	NS	NS	NS	NS
	SE	0.002	0.005	-	0.005	0.005	-	-	-	-	-
8		**Intercept**	**CR**	**HT**	**TS**	**CR²**	**HT²**	**TS²**	**CR·HT**	**CR·TS**	**HT·TS**
Hardness (Newton)	**EE**	68.36	28.76	–7.086	16.437	9.575	NS	NS	NS	11.66	NS
	SE	0.854	1.548	1.548	1.548	1.52	-	-	-	2.023	-
Springiness (ratio)	**EE**	0.918	0.04	NS	0.032	−0.041	−0.022	−0.054	−0.071	−0.033	NS
	SE	0.006	0.007	-	0.007	0.007	0.007	0.007	0.009	0.009	-
Cohesiveness (ratio)	**EE**	0.344	–0.129	NS	0.032	0.028	NS	NS	NS	NS	NS
	SE	0..004	0.007	-	0.007	0.007	-	-	-	-	-
Resilience (ratio)	**EE**	0.109	−0.076	−0.007	0.025	0.019	NS	NS	NS	NS	NS
	SE	0.001	0.002	0.002	0.002	0.002	-	-	-	-	-

CR compression rate (%), *EE* effects estimates, *HT* holding time (s), *NS* non-significative ($p > 0.05$), *SE* standard error (pure), *TS* test speed (mm/s)

Table 7 Stability zones achieved for each day and texture instrumental property for tilapia fillets stored at 4.0 ± 0.1 °C for 8 days

Property	Day			
	0	4	8	Stability zone by property
Hardness	-	1–9 s HT 0.3–1.5 mm/s TS	45–60% CR 0.3–2 mm/s TS	45–60% CR 1–9 s HT 0.3–1.5 mm/s TS
Springiness	60–75% CR 2–5 s HT	-	55–75% CR	55–75% CR 2–5 s HT
Cohesiveness	65–76.8% CR 0.3–2 mm/s TS	65–76.8% CR 0.3–2.5 mm/s TS	68–76.8% CR 0.3–2 mm/s TS	68–76.8% CR 0.3–2 mm/s TS
Resilience	65–76.8% CR 0.3–2 mm/s TS	67–76.8% CR 0.5–2.5 mm/s TS	64–76.8% CR 0.3–2.5 mm/s TS	67–76.8% CR 0.5–2 mm/s TS
Stability zone by day	65–75% CR 2–5 s HT 0.3–2 mm/s TS	67–76% CR 1–9 s HT 0.5–2.5 mm/s TS	68–75% CR 0.3–2 mm/s TS	60–75% CR 2–5 s HT 0.5–2 mm/s TS

CR compression rate, *HT* holding time, *TS* test speed

and 6 s of HT and 50 and 76.8% of CR, springiness values presented a range of 0.80–0.83 (Fig. 3A). Furthermore, in a smaller range between 2 and 5 s of HT and 60 and 75% of CR, the behavior of the level's curve is slightly parallel to the HT axis; it seems that the springiness values (around 0.8) suffer a lower effect of quadratic HT. These findings are supported by Boughattas et al. (2020) who applied 5 s of HT to assess the instrumental texture of sturgeon (*Acipenser gueldenstaedtii*). The same authors found a similar range of instrumental springiness (0.81 to 0.90) during storage with no significant difference between them.

Cohesiveness was mainly negatively affected by linear CR (Table 6) ($p < 0.05$), indicating that cohesiveness has an opposite behavior to hardness. Thus, cohesiveness tends to decrease and increase as an increase in the employed CR and TS, respectively. This behavior

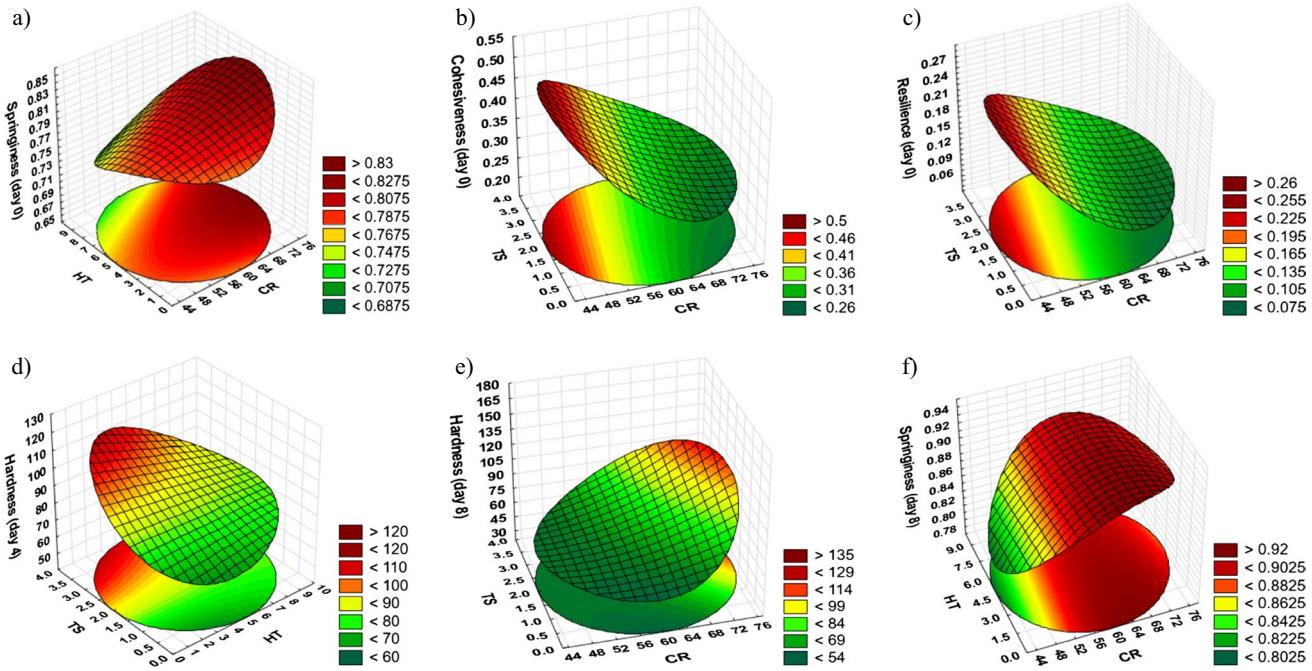

Fig. 3 Response surface graphs of tilapia fillets showing (**a**) the effects of CR and HT on springiness (ratio) at the start of storage, (**b**) the effects of CR and TS on cohesiveness (ratio) at the start of storage, (**c**) the effects of CR and TS on resilience (ratio) at the start of storage, (**d**) the effects of HT and TS on hardness (N) at the middle of storage, (**e**) the effects of CR and TS on hardness (N) at the end of storage, and (**f**) the effects of CR and HT on springiness (ratio) at the end of storage. CR compression rate (%), HT holding time (s), and TS test speed (mm/s)

can be elucidated due to the lower structural damage of the fillet caused by higher TSs, allowing a greater compression area in the second cycle (A2) (Fig. 1). This finding can be well-correlated with the literature. Wu et al. (2018) and Tang et al. (2019) applied 70% and 80% CR, respectively, to assess the instrumental texture of fish fillets. The results found by Wu et al. (2018) ranged from 0.68 to 0.72, while Tang et al. (2019) showed results below 0.6. On the other hand, as exhibited in Fig. 3B, in CRs above 60%, the behavior of the level's curve changes and begins to be parallel to the CR axis. In this way, at higher CRs, TS appears to be responsible for increasing cohesiveness values, which tend to rise as TS increases. In addition, in a range of 65 to 76.8% of CR and 0.3 to 2 mm/s of TS, there is a stability zone, where the results vary minimally, from 0.30 to 0.25 (Table 7). At least, resilience presented a behavior similar to cohesiveness, being negatively affected by linear CR, the main factor influencing this characteristic (Table 6) ($p < 0.05$). Therefore, the results found for instrumental resilience support the findings for cohesiveness, that there is a stability zone in the range between 65 and 76.8% of CR and 0.3 and 2 mm/s of TS on the initial day of storage (Fig. 3C). Moreover, in general, the resilience results decreased as the applied CR increased. Lin et al. (2012) used 30% of CR to assess the instrumental resilience of grass carp fillets (*Ctenopharyngodon idella*) and found values ranging from 0.39 to 0.49. On the other hand, Iaconisi et al. (2017) employed a CR of 50% to evaluate the instrumental texture of blackspot seabream (*Pagellus bogaraveo*) and achieved a resilience value 0.02.

Day 4

Linear CR remained as the main factor affecting hardness (Table 6) ($p < 0.05$). However, different from day 0, other factors, such as linear HT, linear TS, and the interaction between HT and TS (Fig. 3D), also showed statistical significance ($p < 0.05$). This unexpected behavior, since hardness corresponds to the first peak force, can be probably attributed to the structural changes suffered by the fillet due to the repeated compression actions of the four analytical replicates performed for each fillet, responsible for permanent deformation (Fig. 4A), or to the sample geometry, as hypothesized in Fig. 4B. The continuous pH drop during rigor mortis is responsible for promoting the activity of proteolytic enzymes (e.g., calpain, cathepsins, and proteasome) in fish fillets (Bahuaud et al. 2010), making proteins prone to the action of endogenous and exogenous enzymes, mainly of microbial origin, during storage under refrigeration (4 °C) (Yu et al. 2018). In this way, the resolution of rigor mortis

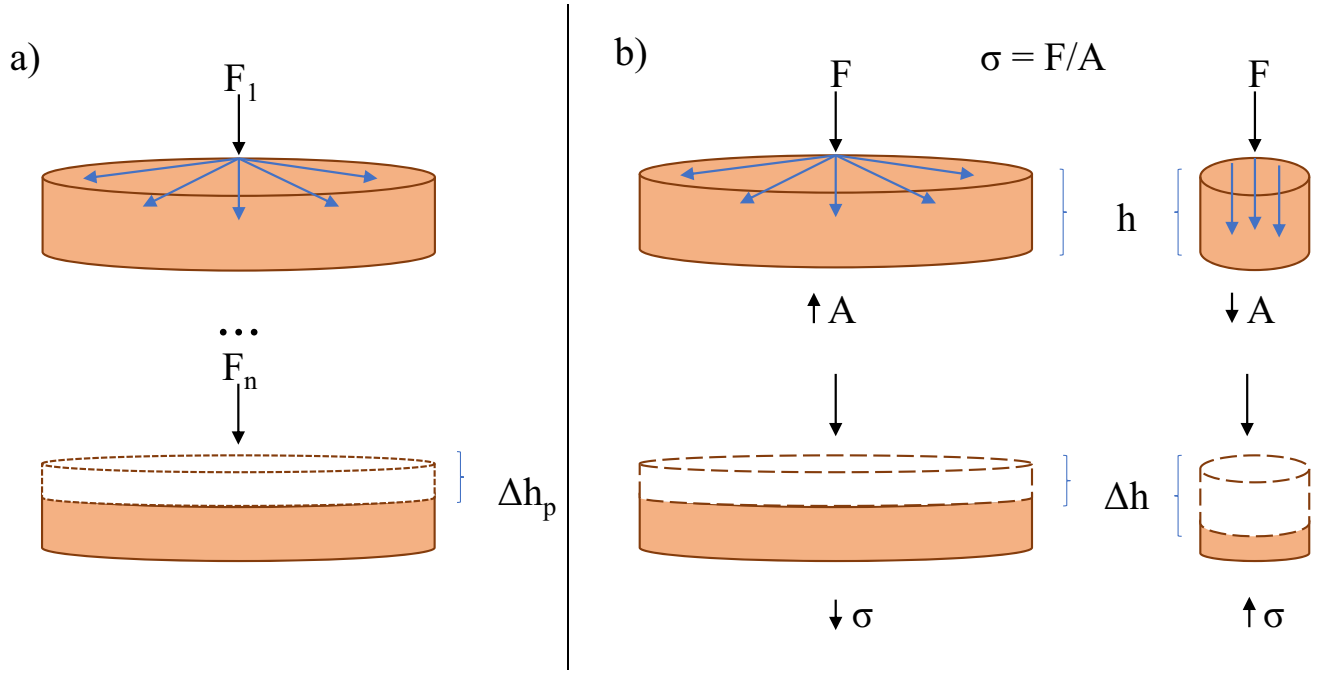

Fig. 4 **a** The effects of repeated uniaxial forces (F_n) applied in a sample together with the biochemical changes of the fillet during the storage results in a retarded recovery process or permanent deformation (Δh_p) that could be responsible by the significative effects of holding time and test speed on hardness values. **b** Hypothetical comparison between the resulting stress (σ) as a ratio of the force (F) and area (A) on two different geometry samples. On samples with higher areas (fillets), the applied force tends to spread through the surface, reducing the deformation (Δh) and probably causing different instrumental property responses from that measured on fish cubes or pieces

and proteolysis of the fish muscles could be responsible for the results achieved on this day.

Springiness, unlike the first day, was not affected by HT, having been influenced mainly by linear CR, followed by the linear TS (Table 6) ($p < 0.05$). Analogous to the first day, cohesiveness and resilience were both affected by linear CR, quadratic CR, and linear TS (Table 6) ($p < 0.05$). Therefore, it appears that areas A1 and A2, and R1 and R2 (Fig. 1) varied similarly during the first half of storage. Moreover, the stability zone achieved was similar to that of the first day (from 65 to 76.8% CR for cohesiveness, and 67 to 76.8% CR for resilience) (Table 7), where the cohesiveness and resilience values obtained varied from 0.3 to 0.25 and from 0.08 to 0.05, respectively. These results are supported by Cropotova et al. (2019), Monteiro et al. (2019), and Sun et al. (2018), who found no significant differences for instrumental cohesiveness of fish species stored under refrigeration during the firsts days of storage.

Day 8

The effects estimated for instrumental texture on the eighth day of storage can be seen in Table 6. For hardness, linear CR remained as the main factor affecting its final values ($p < 0.05$). In addition, quadratic CR and the interaction between CR and TS were also significant ($p < 0.05$), unlike the interaction between HT and TS, which, different from day 4, did not significantly affect hardness ($p < 0.05$). At this point of storage (final days), there is an advanced protein degradation, wherein cathepsins B and L (lysosomal acidic proteinases) are mainly responsible for the proteolysis process (Bahuaud et al. 2010). These endogenous proteinases degrade the main constituents of muscle bands (e.g., desmin, actin, troponin, and tropomyosin) (Delbarre-Ladrat et al. 2004), causing tenderization of fish fillets, making them less rigid and no longer elastic (Cheret et al. 2007). The tenderization process is characterized by the gradual disintegration of the extracellular matrix, where the links between the cytoskeleton and the sarcomeres are the main degraded structures (Delbarre-Ladrat et al. 2006). Therefore, metabolic (e.g., drop in pH and degradation of amino acids) and structural (e.g., proteolysis of actin, myosin, and other sarcoplasmic proteins) changes may justify the reduction in hardness values found during the postmortem period in this study and the literature (Rodrigues et al. 2017; Monteiro et al. 2019; Boughattas et al. 2020). Also, these changes could be related to the higher number of significant effects achieved on the eighth day of storage. Besides, as shown in Fig. 3E, at low CR values (< 60%) and low TS values (< 2 mm/s), a zone could be achieved, in which hardness values vary between 54 and 74 N, characterizing greater reliability and representativeness of the results (Table 7).

Springiness seems to have been influenced by the same process of hardness. Thus, the linear HT and the interaction between HT and TS were the only factors that did not significantly affect this property ($p < 0.05$). On the other hand, as shown in Table 6, the interaction between CR and HT was the most critical factor, affecting springiness negatively ($p < 0.05$). Figure 3F presents the level's curve for springiness on the eighth day of storage. The level's curve starts with a behavior parallel to the HT axis, indicating that for low CRs (from 43.2 to 55%), the increase in springiness occurs due to the application of higher CRs. However, the behavior of the level's curve changes to CR values above 55%, ceasing to be parallel to the HT axis. This new behavior indicates that the application of higher HT has a negative influence on the springiness values, which show regressive quadratic reductions as HT increases. Also, it is correct to state that CR values between 55 and 75% are the most suitable to apply in the final days of storage, since in this range the springiness results vary between 0.90 and 0.92, regardless of the employed HT. Cohesiveness and resilience, as expected, were both affected by the same factors as in previous days (linear CR, quadratic CR, and linear TS) ($p < 0.05$). In this way, a stability zone similar to that found in the previous days (Fig. 3B and C) was reached (Table 7). Therefore, it is correct to state that for cohesiveness, the CR values most suitable to be applied throughout the whole storage should vary in a range from 68 to 76.8%. On the other hand, this same stability zone seems to present a greater range for resilience, between 67 and 76.8%.

Practical Application and Perspectives

Currently, there is no standardization for instrumental texture evaluation of fish fillets. The Research Guidelines proposed by the American Meat Science Association refers solely to (i) meat tenderness of the whole muscle by using the Warner–Bratzler Shear Force (WBSF), and to (ii) compression indices of ground beef, by measuring hardness, springiness, cohesiveness, gumminess, and chewiness, applying a test speed of 100 mm/min and compressing the samples to 70% of their original size (AMSA 2016). Therefore, the stability zones achieved for each property in this study fill the literature gap in addressing the standards for TPA mechanical parameter settings, which is crucial to applying this methodology for assessing the quality of fish fillets. As shown in Table 7, we propose an intersection zone with the most representative values for CR (60–75%), HT (2–5 s), and TS (0.5–2 mm/s), based on their significant effects (linear, quadratic, and interaction) during storage. These findings partially agree with the conclusions of Rosenthal (2010), who recommended the use of CRs above 75% and TS above 2 mm/s. The differences can be justified by (i) the composition of the matrix,

since this author used stable glycerol gels as samples; (ii) the absence of time between the two compressions, as no holding time was considered in the analyses; and (iii) the quadratic and interaction effects between the factors that have not been evaluated. On the other hand, as stated by Szczesniak (2002) and reviewed by Nishinari and Fang (2018), food texture characteristics can be divided into three classes: (i) mechanical, (ii) geometrical, and (iii) composition. In this study, we only evaluated data related to the mechanical characteristics (primary texture properties) and how the texturometer settings can affect the results. Thus, it is reasonable to state that other factors, such as size, weight, thickness, and format of the samples (uniform characteristics of the fish fillets in this study) should also be standardized to obtain rational definitions of the texture of a food matrix. Therefore, further studies could be performed to assess the influence of these geometric and compositional parameters on the results of the mechanic characteristics evaluated by TPA.

Conclusion

Due to the metabolic and biochemical changes that occur in the fish fillets during storage, all the tested factors significantly affected the instrumental texture at some time of the storage. Through the application and analysis of the model, we can state that (i) linear CR was the main factor affecting all properties significantly in all storage days. (ii) Cohesiveness and resilience presented similar behavior to each other during the 8 days, and the most suitable CR and TS values for these properties were around 64 to 76.8% and 0.3 to 2.5 mm/s, respectively. (iii) HT was a critical factor affecting springiness during the whole storage, linearly, quadratically, or by interaction. (iv) Two stability zones were achieved for springiness, at the start of storage (CR between 60 and 75% and HT between 2 and 5 s) and on the final day (CR values from 55 to 75%). (v) The interaction between CR and TS significantly affected hardness only on the last day of storage, in which similar results for this characteristic were found at low CR values (< 60%) and low TS values (< 2 mm/s).

This study proves that CR, HT, and TS are factors that differently affect the instrumental texture results. Furthermore, we can conclude that the most suitable TPA settings are in the range of 60–75% of CR, 2–5 s of HT, and 0.5–2.0 mm/s of TS, in which more reliable and representative results could be achieved, optimizing the use of a texturometer as a tool for fish quality control. Therefore, through our results, it would be possible to establish some standards for the use of TPA, considering CR, HT, and TS, for quality assessment of fish fillets, providing more accurate and representative responses for instrumental texture of the fish samples.

Funding This study was funded by the Fundação de Amparo à Pesquisa do Estado do Rio de Janeiro (FAPERJ) Brazil—grant numbers (E-26/203.049/2017 and E-26/200.195/2020), the Conselho Nacional de Desenvolvimento Científico e Tecnológico (CNPq)—grant number (311422/2016-0), and the Coordenação de Aperfeiçoamento de Pessoal de Nível Superior (CAPES) Brazil-Finance Code 001.

Declarations

Ethical Approval This article does not contain any studies with human or animal participants performed by any of the authors. The authors have obtained the whole fish fillets directly from the slaughterhouse for the work.

Informed Consent Not applicable.

Conflict of Interest Yago A A Bernardo declares that he has no conflict of interest. Denes K A Rosário declares that he has no conflict of interest. Maria Lúcia G Monteiro declares that she has no conflict of interest. Sérgio B Mano declares that he has no conflict of interest. Isabella F Delgado declares that she has no conflict of interest. Carlos A Conte-Junior declares that he has no conflict of interest.

References

American Meat Science Association (AMSA) (2016) Research guidelines for cookery, sensory evaluation and instrumental tenderness measurements of fresh meat, 2nd edn. Champaign, USA, 105 p

Aslan N (2008) Application of response surface methodology and central composite rotatable design for modeling and optimization of a multi-gravity separator for chromite concentration. Powder Technol 185:80–86. https://doi.org/10.1016/j.powtec.2007.10.002

Bahuaud D, Gaarder M, Veiseth-Kent E, Thomassen M (2010) Fillet texture and protease activities in different families of farmed Atlantic salmon (Salmo salar L.). Aquaculture 310:213–220. https://doi.org/10.1016/j.aquaculture.2010.10.008

Baranyi J, Pin C, Ross T (1999) Validating and comparing predictive models. Int J Food Microbiol 48:159–166. https://doi.org/10.1016/S0168-1605(99)00035-5

Baş D, Boyacı İH (2007) Modeling and optimization I: usability of response surface methodology. J Food Eng 78:836–845. https://doi.org/10.1016/j.jfoodeng.2005.11.024

Borges A, Conte-Junior CA, Franco RM, Freitas MQ (2013) Quality Index Method (QIM) developed for pacu Piaractus mesopotamicus and determination of its shelf life. Food Res Int 54:311–317. https://doi.org/10.1016/j.foodres.2013.07.012

Boughattas F, Vilkova D, Kondratenko E, Karoui R (2020) Targeted and untargeted techniques coupled with chemometric tools for the evaluation of sturgeon (Acipenser gueldenstaedtii) freshness during storage at 4 °C. Food Chem 312:126000. https://doi.org/10.1016/j.foodchem.2019.126000

Bourne MC (1968) Texture profile of ripening pears. J Food Science 33:223–226. https://doi.org/10.1111/j.1365-2621.1968.tb01354.x

Box GEP, Wilson KB (1951) On the experimental attainment of optimum conditions. J Roy Stat Soc 13:1–45. https://doi.org/10.1111/j.2517-6161.1951.tb00067.x

Bruni L, Belghit I, Lock E et al (2020) Total replacement of dietary fish meal with black soldier fly (*Hermetia illucens*) larvae does not impair physical, chemical or volatile composition of farmed Atlantic salmon (*Salmo salar* L.). J Sci Food Agric 100:1038–1047. https://doi.org/10.1002/jsfa.10108

Casas C, Martinez O, Guillen MD et al (2006) Textural properties of raw Atlantic salmon (Salmo salar) at three points along the fillet, determined by different methods. Food Control 17:511–515. https://doi.org/10.1016/j.foodcont.2005.02.013

Cheng J-H, Sun D-W, Zhu Z (2017) Effects of frozen storage condition abuse on the textural and chemical properties of grass carp (*Ctenopharyngodon idella*) fillets: frozen conditions on textural and chemical properties of fish. J Food Process Preserv 41:e13002. https://doi.org/10.1111/jfpp.13002

Cheret R, Delbarreladrat C, Lamballerieanton M, Verrezbagnis V (2007) Calpain and cathepsin activities in post mortem fish and meat muscles. Food Chem 101:1474–1479. https://doi.org/10.1016/j.foodchem.2006.04.023

Cropotova J, Mozuraityte R, Standal IB et al (2019) Superchilled, chilled and frozen storage of Atlantic mackerel (*Scomber scombrus*) fillets – changes in texture, drip loss, protein solubility and oxidation. Int J Food Sci Technol 54:2228–2235. https://doi.org/10.1111/ijfs.14136

de Bonfim B, C, Monteiro MLG, Santos AFGN do, et al (2020) Nutritional improvement and consumer perspective of fish nuggets with partial substitution of wheat flour coating by fish (Priacanthus arenatus, Cuvier, 1829) waste flour. J Aquat Food Prod Technol 29:28–42. https://doi.org/10.1080/10498850.2019.1693462

Delbarre-Ladrat C, Verrez-Bagnis V, Noël J, Fleurence J (2004) Relative contribution of calpain and cathepsins to protein degradation in muscle of sea bass (Dicentrarchus labrax L.). Food Chem 88:389–395. https://doi.org/10.1016/j.foodchem.2004.01.053

Delbarre-Ladrat C, Chéret R, Taylor R, Verrez-Bagnis V (2006) Trends in postmortem aging in fish: understanding of proteolysis and disorganization of the myofibrillar structure. Crit Rev Food Sci Nutr 46:409–421. https://doi.org/10.1080/10408390591000929

Durmuş M, Surówka K, Ozogul F et al (2017) The impact of gravading process on the quality of carp fillets (Cyprinus carpio): sensory, microbiological, protein profiles and textural changes. J Consum Prot Food Saf 12:147–155. https://doi.org/10.1007/s00003-017-1106-0

Food and Agriculture Organization of the United Nations (FAO) (2020) The state of world fisheries and aquaculture – meeting the sustainable development goals. Rome, 208 p

Granato D, de Araújo Calado VM, Jarvis B (2014) Observations on the use of statistical methods in Food Science and Technology. Food Res Int 55:137–149. https://doi.org/10.1016/j.foodres.2013.10.024

Harimana Y, Tang X, Xu P et al (2019) Effect of long-term moderate exercise on muscle cellularity and texture, antioxidant activities, tissue composition, freshness indicators and flavor characteristics in largemouth bass (Micropterus salmoides). Aquaculture 510:100–108. https://doi.org/10.1016/j.aquaculture.2019.05.051

Iaconisi V, Marono S, Parisi G et al (2017) Dietary inclusion of Tenebrio molitor larvae meal: effects on growth performance and final quality treats of blackspot sea bream (Pagellus bogaraveo). Aquaculture 476:49–58. https://doi.org/10.1016/j.aquaculture.2017.04.007

Jiang Q, Han J, Gao P et al (2018) Effect of heating temperature and duration on the texture and protein composition of Bighead Carp (*Aristichthys nobilis*) muscle. Int J Food Prop 21:2110–2120. https://doi.org/10.1080/10942912.2018.1489835

Lazo O, Guerrero L, Alexi N et al (2017) Sensory characterization, physico-chemical properties and somatic yields of five emerging fish species. Food Res Int 100:396–406. https://doi.org/10.1016/j.foodres.2017.07.023

Li D-Y, Huang Y, Wang K-X et al (2018) Microstructural characteristics of turbot (*Scophthalmus maximus*) muscle: effect of salting and processing. Int J Food Prop 21:1291–1302. https://doi.org/10.1080/10942912.2018.1460758

Liang XF, Hu L, Dong YC et al (2017) Substitution of fish meal by fermented soybean meal affects the growth performance and flesh quality of Japanese seabass (Lateolabrax japonicus). Anim Feed Sci Technol 229:1–12. https://doi.org/10.1016/j.anifeedsci.2017.03.006

Lin W-L, Zeng Q-X, Zhu Z-W, Song G-S (2012) Relation between protein characteristics and TPA texture characteristics of crisp grass carp (Ctenopharyngodon idellus C. Et V) and grass carp (Ctenopharyngodon idellus): texture-protein. J Texture Stud 43:1–11. https://doi.org/10.1111/j.1745-4603.2011.00311.x

Monteiro ML, Mársico ET, Rosenthal A, Conte-Junior CA (2019) Synergistic effect of ultraviolet radiation and high hydrostatic pressure on texture, color, and oxidative stability of refrigerated tilapia fillets. J Sci Food Agric 99:4474–4481. https://doi.org/10.1002/jsfa.9685

Moriya K, Nakazawa N, Osako K, Okazaki E (2019) Effect of subzero temperature treatment at −2 °C before thawing on prevention of thaw rigor, biochemical changes and rate of ATP consumption in frozen chub mackerel (Scomber japonicus). LWT 114:108396. https://doi.org/10.1016/j.lwt.2019.108396

Nishinari K, Fang Y (2018) Perception and measurement of food texture: solid foods. J Texture Stud 49:160–201. https://doi.org/10.1111/jtxs.12327

Nishinari K, Fang Y, Rosenthal A (2019) Human oral processing and texture profile analysis parameters: bridging the gap between the sensory evaluation and the instrumental measurements. J Texture Stud 50:369–380. https://doi.org/10.1111/jtxs.12404

Patras A, Tiwari B, Brunton N, Butler F (2009) Modelling the effect of different sterilisation treatments on antioxidant activity and colour of carrot slices during storage. Food Chem 114:484–491. https://doi.org/10.1016/j.foodchem.2008.09.104

Pavón Y, Cian RE, Campos Soldini MA et al (2018) Sensory and instrumental textural changes in fillets from Pacú (*Piaractus mesopotamicus*) fed different diets. J Texture Stud 49:646–652. https://doi.org/10.1111/jtxs.12372

Peleg M (2019) The instrumental texture profile analysis revisited. J Texture Stud 50:362–368. https://doi.org/10.1111/jtxs.12392

Roco T, Torres MJ, Briones-Labarca V et al (2018) Effect of high hydrostatic pressure treatment on physical parameters, ultrastructure and shelf life of pre- and post-rigor mortis palm ruff (Seriolella violacea) under chilled storage. Food Res Int 108:192–202. https://doi.org/10.1016/j.foodres.2018.03.009

Rodrigues BL, da Costa MP, da Silva FB et al (2017) Instrumental texture parameters as freshness indicators in five farmed Brazilian freshwater fish species. Food Anal Methods 10:3589–3599. https://doi.org/10.1007/s12161-017-0926-y

Rosario DKA, Bernardo YAA, Mutz YS et al (2019) Modelling inactivation of Staphylococcus spp. on sliced Brazilian dry-cured loin with thermosonication and peracetic acid combined treatment. Int J Food Microbiol 309:108328. https://doi.org/10.1016/j.ijfoodmicro.2019.108328

Rosenthal AJ (2010) Texture profile analysis - how important are the parameters?: Parameters in texture profile analysis. J Texture Stud 41:672–684. https://doi.org/10.1111/j.1745-4603.2010.00248.x

Ross T (2000) Predictive modelling of the growth and survival of Listeria in fishery products. Int J Food Microbiol 62:231–245. https://doi.org/10.1016/S0168-1605(00)00340-8

Singh A, Benjakul S (2018) Proteolysis and its control using protease inhibitors in fish and fish products: a review: proteolysis-control in fish/fish product. Comp Rev Food Sci Food Saf 17:496–509. https://doi.org/10.1111/1541-4337.12337

Smith EP, Rose KA (1995) Model goodness-of-fit analysis using regression and related techniques. Ecol Model 77:49–64. https://doi.org/10.1016/0304-3800(93)E0074-D

Sreelakshmi KR, Rehana R, Renjith RK et al (2019) Quality and shelf life assessment of puffer fish (*Lagocephalus guentheri)* fillets during chilled storage. J Aquat Food Prod Technol 28:25–37. https://doi.org/10.1080/10498850.2018.1559905

Sun Y, Ma L, Ma M et al (2018) Texture characteristics of chilled prepared Mandarin fish (*Siniperca chuatsi*) during storage. Int J Food Prop 21:242–254. https://doi.org/10.1080/10942912.2018.1451343

Szczesniak AS (2002) Texture is a sensory property. Food Qual Prefer 13:215–225. https://doi.org/10.1016/S0950-3293(01)00039-8

Tang M, Dai H, Ma L et al (2019) Degradation of structural proteins and their relationship with the quality of Mandarin fish (*Siniperca chuatsi*) during post-mortem storage and cooking. Int J Food Sci Technol ijfs.14421. https://doi.org/10.1111/ijfs.14421

te Giffel MC, Zwietering MH (1999) Validation of predictive models describing the growth of Listeria monocytogenes. Int J Food Microbiol 46:135–149. https://doi.org/10.1016/S0168-1605(98)00189-5

Wang X, Shan J, Han S et al (2019) Optimization of fish quality by evaluation of total volatile basic nitrogen (TVB-N) and texture profile analysis (TPA) by near-infrared (NIR) hyperspectral imaging. Anal Lett 52:1845–1859. https://doi.org/10.1080/00032719.2019.1571077

Wu F, Wen H, Tian J et al (2018) Effect of stocking density on growth performance, serum biochemical parameters, and muscle texture properties of genetically improved farm tilapia, Oreochromis niloticus. Aquacult Int 26:1247–1259. https://doi.org/10.1007/s10499-018-0281-z

Xu Y, Liu Y, Zhang C et al (2016) Physicochemical responses and quality changes of turbot (*Psetta maxima*) during refrigerated storage. Int J Food Prop 19:196–209. https://doi.org/10.1080/10942912.2015.1022260

Yang S, Li L, Qi B et al (2015) Quality evaluation of crisp grass carp (Ctenopharyngodon idellus C. ET V) based on instrumental texture analysis and cluster analysis. Food Anal Methods 8:2107–2114. https://doi.org/10.1007/s12161-015-0101-2

Yu D, Regenstein JM, Zang J et al (2018) Inhibitory effects of chitosan-based coatings on endogenous enzyme activities, proteolytic degradation and texture softening of grass carp (Ctenopharyngodon idellus) fillets stored at 4 °C. Food Chem 262:1–6. https://doi.org/10.1016/j.foodchem.2018.04.070